Open Access **Baghdad Science Journal** **P-ISSN: 2078-8665**
Published Online First: January 2021 **E-ISSN: 2411-7986**

DOI: http://dx.doi.org/10.21123/bsj.2021.18.2.0409

The Energy Spectra and Heat Capacity of GaAs Gaussian Quantum Dot in an External Magnetic Field

Mahmoud Ali ***Mohammad Elsaid**** ***Ayham Shaer***

Department of Physics, Faculty of Science, An- Najah National University, Nablus, West Bank, Palestine
Corresponding author: mkelsaid@najah.edu,mahmoud.ali@najah.edu,ayham.shaer@najah.edu
ORCID ID: https://orcid.org/0000-0002-1392-3192,https://orcid.org/0000-0002-3738-5851, https://orcid.org/0000-0002-6518-6470

Received 19/2/2020, Accepted 4/11/2020, Published Online First11/1/2021, Published 1/6/2021

Abstract:

In this paper, a theoretical study of the energy spectra and the heat capacity of one electron quantum dot with Gaussian Confinement in an external magnetic field are presented. Using the exact diagonalization technique, the Hamiltonian of the Gaussian Quantum Dot (GQD) including the electron spin is solved. All the elements in the energy matrix are found in closed form. The eigenenergies of the electron were displayed as a function of magnetic field, Gaussian confinement potential depth and quantum dot size. Explanations to the behavior of the quantum dot heat capacity curve, as a function of external applied magnetic field and temperature, are presented.

Key words: Energy spectra, Exact diagonalization technique, Gaussian quantum dot, Heat capacity.

Introduction:

In the last years, the study of low dimensional systems, especially quantum dot (QD) has gotten a great interest because of their unique physical properties and great device applications like lasers, single electron transistors, quantum dot solar cells, and quantum computers (1-6). Application of a magnetic field normal to the plane of the quantum dot leads to an additional contribution to the system spectra and correlation effects of the interactive electrons in a QD.

Various studies solved the QD-Hamiltonian with parabolic harmonic confinement potential by using several techniques. The variational technique was used to study the quantum dot system (7-10). The general closed-form for parabolic QD solution was obtained by Kandemir (11-12). Elsaid solved the quantum dot Hamiltonian for two interacting electrons using 1/N method (13-14). In Reference (15), the authors used the multi-parameter variational method to find the energy spectra for two interacting electrons in QD. Many authors have investigated the energy spectra for low dimensional system taking into consideration the effect of external field (16-19).

Gaussian potential is an effective potential in many branches of theoretical physics. Gaussian QD has been investigated approximately for one particle problem by different authors (20-28). The variational and numerical diagonalization techniques have been applied to study the QD Hamiltonian, and investigate the electronic structure, magnetic and thermodynamic properties of a single (29-31) and coupled quantum dots (32-34).

This work aims to study the energy spectra and thermal properties of an electron confined in a quantum dot with Gaussian potential under the effects of an external magnetic field. The effects of different QD radii (R), potential depth (V_0), the external magnetic field, and temperature (T), the average thermal energy of the electron in a Gaussian quantum dot (GQD) have been investigated. Moreover, the heat capacity behavior of the (GQD), as a function of a uniform external magnetic field and temperature has been explained. The rest of paper is organized as follows: The Hamiltonian theory and computational procedures of single electron confined in GQD have been given. Next, the authors exhibit how to calculate the heat capacity using the average energy expression. The final part will be dedicated to the numerical results and conclusion.

Theory

There are three main parts in the theory: The two-dimension Hamiltonian, the numerical diagonalization method and the heat capacity.

The quantum dot Hamiltonian

The Hamiltonian of one electron confined in QD in presence of Gaussian confinement potential and uniform external magnetic field is set as (35),

$$\widehat{H} = \frac{1}{2m*}\left(\vec{P} - \frac{|e|}{c}\vec{A}\right)^2 - V_0 e^{-(\rho^2/2R^2)} \quad (1)$$

Where $\vec{P}$ is the momentum , $\vec{\rho}$the position vector of an electron, m^* is the effective mass of the electron, $\vec{A}$ is the vector potential related to the external magnetic field $\vec{B}$along z-direction and, V_0 is the confining potential depth which is taken as Gaussian potential,

The Hamiltonian can be expressed as,

$$\widehat{H} = -\frac{\hbar^2}{2m^*}\nabla_\rho^2 + V(\rho) + \frac{1}{2}m^*{\omega_c}^2\rho^2 + \frac{1}{2}\hbar\omega_c\left(\widehat{L}_z + g^*\widehat{S}_z\right) \quad (2)$$

where $\hat{L}_z$ is the z-component of the electron angular momentum, ω_c is the cyclotron frequency given by $\omega_c = eB/m^*$, B is the magnetic field strength, R is the radius of the quantum dot,V_0 is the confining potential depth and the effective Lande g- factor for GaAs denotes by g* (g*= -0.44).

Exact diagonalization technique

The presence of the Gaussian potential term in the system Hamiltonian makes the analytical solution not possible. Therefore, the exact diagonalization technique has been used to obtaining Hamiltonian solution. The bases are taken to be Fock-Darwin states (36), set as, $|nm_z>$.

$$|nm_z> = \frac{\alpha}{\sqrt{\pi}}\left(\frac{n!}{(n+|m_z|)!}\right)^{\frac{1}{2}}(\alpha\rho)^{|m_z|} m\, L_n^{|m_z|}(\alpha^2\rho^2)e^{\frac{-1}{2}\alpha^2\rho^2}e^{im_z\phi}\chi(\sigma) \quad (3)$$

With $\alpha = \sqrt{\frac{\omega\, m^*}{\hbar}}$, n and m_z are the radial quantum number and the azimuthal quantum number, respectively, where $\chi(\sigma)$ is the spin operator $\hat{S}_z$ eigenstate and , $L_n^{|m_z|}$ is the known associated Laguerre polynomial.

The Hamiltonian can be written as $\widehat{H} = \widehat{H}_0 + \widehat{H}_1$ where,

$$\widehat{H}_0 = -\frac{\hbar^2}{2m^*}\nabla_\rho^2 + \frac{1}{2}m^*\omega^2\rho^2 + \frac{1}{2}\hbar\omega_c\left(\hat{L}_z + g^*\widehat{S}_z\right) \quad (4)$$

$$\widehat{H}_1 = -\frac{1}{2}m^*\omega_0^2\rho^2 - V_0 e^{-(\rho^2/2R^2)} \quad (5)$$

and ω^2 is the effective frequency, defined as $\omega^2 = \omega_0^2 + \frac{1}{4}\omega_c^2$,

where $\widehat{H}_0$ represents the harmonic oscillator Hamiltonian with renowned eigenstates $|\, n\, m_z\rangle$ and energies

$$E_n = (2n + |m_z| + 1)\,\hbar\omega + \frac{1}{2}\hbar\,\omega_C\,(m_z + g^*S_z). \quad (6)$$

one can use these bases $|\, n\, m_z\rangle$ to write the matrix elements of the Hamiltonian $\widehat{H}$, as,

$$\langle \acute{n}\ m_z|\widehat{H}|n\ m_z\rangle = \langle \acute{n}\ m_z|\widehat{H}_0|n\ m_z\rangle + \langle \acute{n}\ m_z|\widehat{H_1}|n\ m_z\rangle = (2n + |m_z| + 1)\,\hbar\omega + \frac{1}{2}\hbar\,\omega_C\,(m_z + g^*S_z) + \langle \acute{n}\ m_z| - V_0 e^{-(\rho^2/2R^2)}|n\ m_z\rangle + \langle \acute{n}\ m_z| - \frac{1}{2}m^*\omega_0^2\rho^2|n\ m_z\rangle \quad (7)$$

Using Laguerre's relation below, the matrix element which represents the Gaussian confinement potential $\langle n'\ m_z\,| - V_0 e^{-(\rho^2/2R^2)}|\ n\ m_z\rangle$can be evaluated in a closed form, using the relation (35),

$$\int_0^\infty e^{-pt}t^{\alpha-1}L_m^\lambda(bt)L_n^\beta(at)dt = \frac{\Gamma(\alpha)p^{-\alpha}(\beta+1)_n\,(\lambda+1)_m}{m!n!}\sum_{j=0}^{m}\frac{(-m)_j(\alpha)_j}{(\lambda+1)_j\,j!}\left(\frac{a}{p}\right)^j\sum_{k=0}^{n}\frac{(j+\alpha)_k(-n)_k}{k!\,(\beta+1)_k}\left(\frac{b}{p}\right)^k \quad (8)$$

Where $(a)_j$ is the Pochhammer function, this analytical form of above integration seriously decreases the computing time required in the diagonalization process and improves the integral accuracy compared with the numerical integration.

The matrix element for the Gaussian potential can be expressed as,

$$\left\langle nm\left|-V_0 e^{-(\rho^2/2R^2)} - \frac{1}{2}m^*\omega_0^2\rho^2\right|n'm'\right\rangle = -V_0\, N_{nm}N_{n'm'}\frac{\Gamma(|m|+1)(|m|+1)_n(|m|+1)_{n'}\times\left(\frac{1}{R^2\left(\frac{\omega_c^2}{4}+\omega_0^2\right)^{.5}}+1\right)^{-|m|-1}}{n!n'!}\times \sum_{j=0}^{n}\frac{\left(\frac{1}{R^2\left(\frac{\omega_c^2}{4}+\omega_0^2\right)^{.5}}+1\right)^{-j}(-n)_j(|m|+1)_j\times\sum_{\kappa=0}^{n'}\frac{\left(\frac{1}{R^2\left(\frac{\omega_c^2}{4}+\omega_0^2\right)^{.5}}+1\right)^{-k}(-n')_\kappa(|m|+j+1)_\kappa}{(|m|+1)_\kappa\kappa!}}{(|m|+1)_j j!} \quad (9)$$

Using the standard procedure for the diagonalization process; the eigenenergies of the QD-system Hamiltonian can be obtained from the condition: $| H - E_n I | = zero$

Statistical energy and Heat capacity.

The computed spectra of the system have been used as essential Input for calculating the statistical average energy as:

$$\langle \mathrm{E}\left(R, V_o, B, T\right)\rangle = \frac{\sum_{\alpha=1}^{\mathrm{N}} \mathrm{E}_\alpha \mathrm{e}^{-\mathrm{E}\alpha/\mathrm{k_B T}}}{\sum_{\alpha=1}^{\mathrm{N}} \mathrm{e}^{-\mathrm{E}\alpha/\mathrm{k_B T}}} \quad . \quad (10)$$

Then, by taking the temperature derivative of $< E >$ one can find the heat capacity,

$$C_v\left(R, V_o, B, T\right) = \frac{\partial\langle \mathrm{E(R, V_0, B, T)}\rangle}{\partial \mathrm{T}} \quad (11)$$

Results and Discussion:

The numerical results for the energy, and heat capacity for GaAs Gaussian quantum dot are presented. Furthermore, the behavior of the sketched heat capacity, as function of magnetic field and temperature, are explained. The material parameters for GaAs medium taken to be m^* =0.067m_0., effective Rydberg R^* =5.83meV and Bohr radius a^* =9.8nm are used as energy and length, respectively. a single electron GQD presented in a uniform external magnetic field is studied. The energy spectra, E_n, are essential input data to calculate the heat capacity. Figures were used to clarify the results.

QD Energy Spectra

The ground state energy for the QD is calculated as a function of the quantum radii (R) at constant potential depth (V_0), as displayed in Fig.1, the figure shows that as the quantum dot radius increases ,the electron ground state energy significantly reduces due to the reduction in the electron confinement energy.

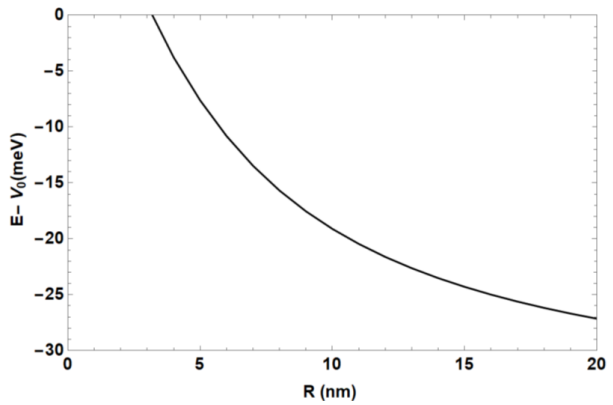

Figure 1. The computed ground state energy of an electron in a quantum dot as a function of the quantum radius, R, at B=0 and V_0=36.7meV

Figure 2 shows the ground state and a few excited states energies of the Gaussian QD as a function of the magnetic field B. The figure shows the effects of the Zeeman splitting and the spin on each level. As the magnetic field increase, the spin and Zeeman terms show considerable energy contribution effects.

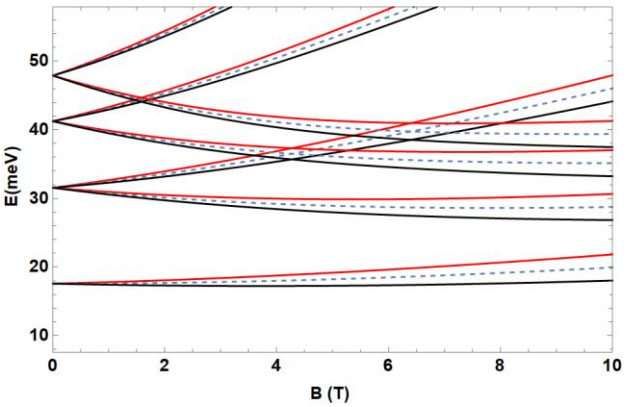

Figure 2. The calculated energies of a single electron GQD versus the magnetic field at R=10 nm and V_0 = 36.7 meV. The black (Red) curve for S=1/2 (−1/2) and the dashed line when the spin has been ignored.

Figure 3 describes the statistical energy ⟨E⟩ as a function of the magnetic field of the GQD, considering the effect of the electron spin term. The figure shows that at low temperature T=5 mK the energy goes down as B increases, since the contribution of the thermal energy is small at low temperatures, whereas the spin term ($\omega_c g^* \hat{S}_z$) is significant and its negative energy contribution reduces the statistical energy, this behavior continues up to B≈4 T, then the energy begins to increase as the magnetic field raises. As the temperature increases, from 5 mK to 10 and 20 K, the curve of the ground state shows a considerable enhancement due to the considerable increment in the contribution of the thermal energy.

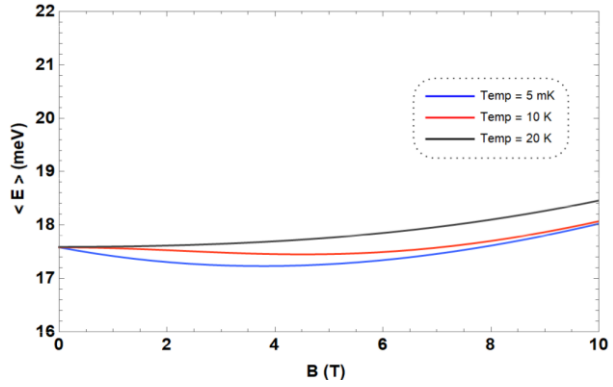

Figure 3. The statistical energy against the magnetic field B at V_0=36.7meV, R=10nm, g*=−0.44, T = 5 mK, 10, and 20 K from bottom to top.

Baghdad Science Journal
P-ISSN: 2078-8665
E-ISSN: 2411-7986

Figure 4 shows the potential depth V_0 effect on the behavior of $\langle E \rangle$ at several temperature values. The figure shows a large change in the behaviors of the energy curves as result of raising of V_0 from: 36.7meV to 100meV. The Gaussian potential term ($-V_0 e^{-\rho^2/2R^2}$) increases greatly the electron ground state energy because of the larger Gaussian energy confinement.

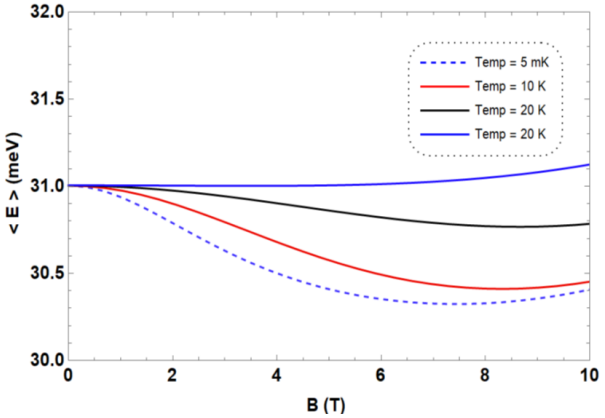

Figure 4. The statistical energy <E> against the magnetic field B at V_0 =100 meV, R=10 nm, g*= −0.44 and T = 5 mK, 10, 20, and 30 K .

Figure 5 shows the dependence of the convergence of the GQD energy spectra on the temperature by plotting $\langle E \rangle$ versus the temperature at constant B=2T, R=10nm and V_0=36.7 meV and different numbers of bases (n) used in the statistical energy summation. It is evident from the figure that quite high number of bases are needed to achieve the stability in our numerical results when the temperature increases, because at higher temperature, the occupation probability of the higher excited states increases, meaning that there is a valuable contribution to higher energy levels in the statistical energy. Therefore, the number of bases must be increased to ensure that higher energy levels are involved in the statistical energy. To obtain a very good numerical stability calculation, the number of bases have been increased to over 90, at high temperature, as shown.

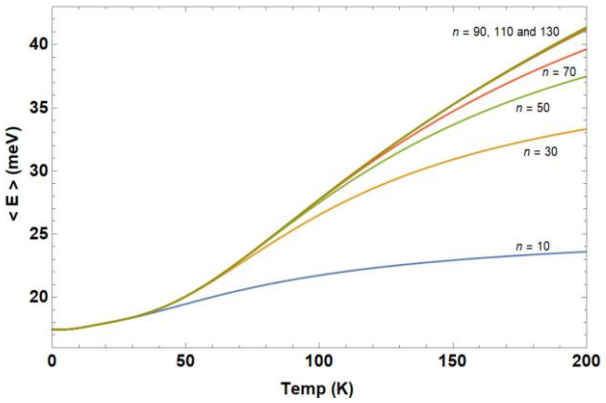

Figure 5. The average thermal energy $< E >$ versus T at V_0 =36.7 meV, R=10nm, g^*= −0.44, B=2T and n = 10, 30, 50,70,90,110 and 130.

Heat capacity

The effects of temperature, confining potential and magnetic field on the heat capacity of single electron in a GaAs Gaussian quantum dot are presented.

Figure 6 exhibits the dependence of C_v on T for fixed values of V_0, quantum dot size R and selected values of B. For all values of magnetic field strengths, the heat capacity approaches to zero as T goes to zero, and the curve shows a peak behavior as the temperature increases, while at high temperature (room temperature) it saturates to the classical limit ($1k_B$). For example, at B= 3T the heat capacity, C_v , starts to rise from the beginning at low temperatures making a peak (is well-known Schottky anomaly, this occurs due to including the spin) and then re-rises as the temperature increases, finally reaching approximate stability. From the figure, one can conclude that the saturation limit becomes quite higher as the magnetic field increases and it reaches $2k_B$. Both behavior-limits of the heat capacity curves are explained later.

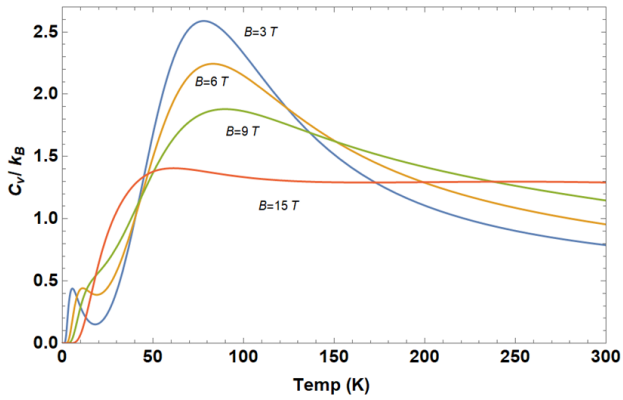

Figure 6. The heat capacity C_v versus temperature T at V_0 =36.7 meV, R=10 nm, g^*= −0.44 and B = 0, 5, 10 and 15T.

Figure 7 shows the effect of the confinement depth V_0 on C_v–T curve by taking

different values of V_0 at particular values of the quantum dot size R, and the magnetic field strength B. From the figure one can distinguish that at low temperatures the C_v– T curve behaves qualitatively the same way for the three different V_0 values to reach the same peak (Schottky). The variation in the heat capacity behavior starts in the decreasing of the C_v after the peak (T=20K). The reason for this variation is mainly due to confinement, since the difference between the two energy levels ΔE increases as the confinement depth enhances, this means lower probability of the electron to be excited by the small available thermal energy. For further temperature increment, the heat capacity starts increasing to show a peak behavior before reaching the saturation.

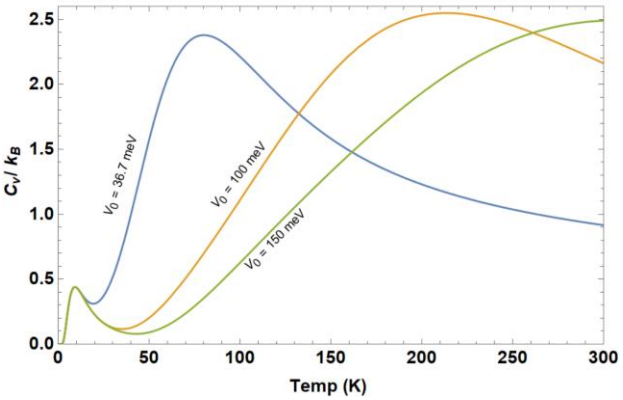

Figure 7. The heat capacity versus the temperature T at R=10 nm, g^*= −0.44, B=5T andV_0 =36.7, 100 and 150 meV.

To explain the difference in the aforementioned saturation limits-behavior, shown previously by the two plots (figure 6 and 7), we compare, in Fig. 8, the Gaussian and parabolic confinements types. The parabolic potential model can be used to approximate the Gaussian potential confinement. This approximation has two advantages: first, it gives an analytic energy expression which provides all the energy spectra including the low-lying state. Second, it makes the role of the magnetic confinement energy part easy to understand, since the proportional quadratic term (ρ^2), due to the magnetic field (as shown in equation 2), is a parabolic type, similar to the parabolic confinement term.

In Fig. 8, the low-lying energies of the electron have been plotted for both Gaussian and its parabolic approximation (using Taylor expansion). In general, the two potentials match each other at small values of radial distance, r, so the ground state energy in both potentials are very close, but for the higher states, one can notice the difference between the two successive states. The parabolic case has larger energy states than the corresponding ones for the Gaussian type. For finite range of energy (0 to 200 meV), the Gaussian confinement provides a greater number of bound states with closer separation than parabolic confinement. In this case, the electron needs less thermal energy to make a transition to higher state compared with corresponding one in the parabolic approximation case. Based on this argument, it is expected to find that the heat capacity curves of the two potential models match each other only at low temperature range. However, at higher temperature range, the Gaussian case shows a higher heat capacity limit as seen in Fig. 9, where the heat capacity curve has been plotted as function of temperature. For high confinement strength case, $V_0 = 200\ meV$, and B= 15 T, the number of available bound states in the Gaussian confinement is enough to ensure the convergence in the heat capacity even at high temperature like T=400K. The quantum dot system, at high temperature and low-magnetic field case (B=3T), is expected to behave as a free two-dimensional system due to the excess thermal energy available as a kinetic energy for the electron .The system expected to have heat capacity limit ($1\ k_B$), with $k_B/2$, for each degree of freedom. However, at high-magnetic field value (B=15T), the strong magnetic field is still confining the electron as parabolic potential type and with a larger heat capacity limit of ($2\ k_B$) for a two-dimensional system with parabolic confinement. The parabolic heterostructure potential term and the magnetic field confinement term will add their energy contributions to give a heat capacity limit of ($2k_B$) for the electron quantum dot system. Figure 9 shows clearly that the heat capacity curve goes to $c_v = 1\ k_B$ at B=3 T and 300K and 2 k_B, at B=15 T and 300K, respectively. The obtained heat capacity limit-cases are in agreement with the discussion given in Ref [37] where the authors have been used the field approximation technique to solve the Gaussian confinement potential.

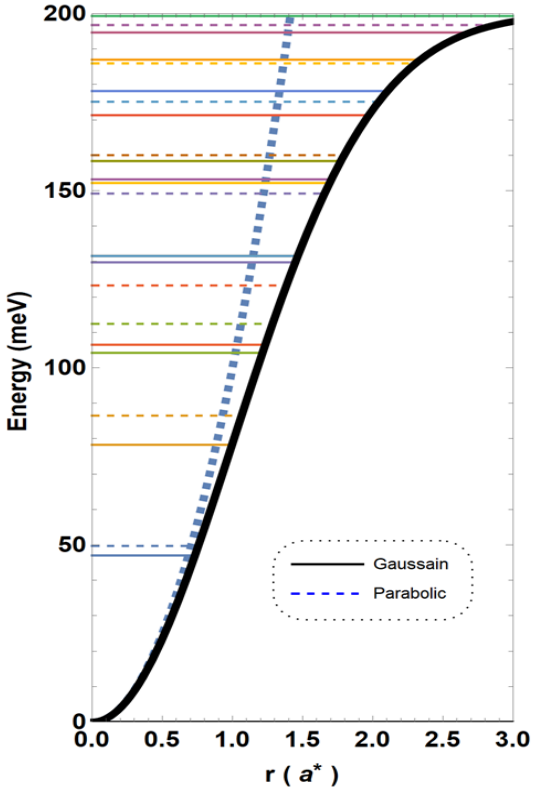

Figure 8. the low-lying energies of the system under the influence of Gaussian confinement compared to parabolic approximation for $V_0 = 200\ meV$, and $R = 10\ nm$,

Recalling back to the discussion of the saturation-limits cases in Fig. 7, where one can see that for low confinement $V_0 = 36.7$, the heat capacity peak value $\approx 2\ k_B$ at T $\approx 100\ K$, this is attributed to the small energy separation in the higher states , but as the temperature increases, the number of bound states in the Gaussian well is limited, so there is a good probability of electron to be excited to free electron saturation case. However, the presence of the small magnetic field confinement (B=5 T) is raising this limit quietly. For higher or strong confinement $V_0 = 100$ and $150\ meV$ cases, the above discussion is still valid but the heat capacity exhibits the 2D parabolic case because the room temperature is not sufficient to fully excite the electron. The electron. in this case, is still bounded by the Gaussian strong potential confinement as a two-dimensional system. While C_v is expected to decrease as the temperature increases. The plot in Fig. 6, clearly shows that the magnetic field pulls the heat capacity saturation to parabolic saturation limit, $2k_B$.

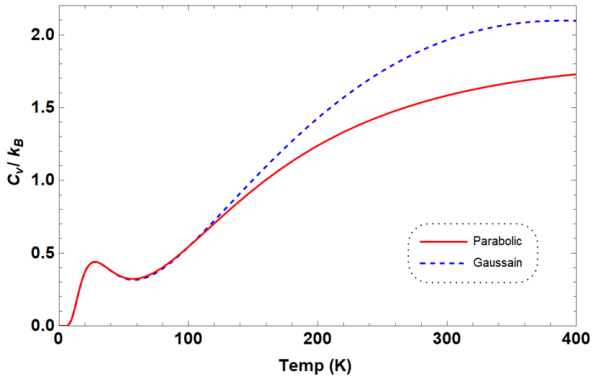

Figure 9. The heat capacity C_v versus the temperature T at R=10 nm, g*= −0.44, B=15T and V_0 = 200 meV.

Conclusion:

The numerical diagonalization technique has been used to solve the QD Hamiltonian and to get the energy and the heat capacity (C_v) of one electron GaAs quantum dot confined by a Gaussian potential as a function of the magnetic field (B), potential depth (V_0), radius (R), and temperature (T). In this work, the dependence of the spectra on the radius has been investigated as an initial step. Furthermore, the statistical energy has been computed, taking into consideration the spin effect. The QD-energies are presented against the physical parameters of the GQD: B, R, V_0 and T. Detailed explanations to the effects of these parameters on the heat capacity curve of the QD have been provided. The heat capacity, as a thermodynamic quantity, shows a considerable dependence on these quantum dot parameters.

Authors' declaration:

- Conflicts of Interest: None.
- We hereby confirm that all the Figures and Tables in the manuscript are mine ours. Besides, the Figures and images, which are not mine ours, have been given the permission for re-publication attached with the manuscript.
- Ethical Clearance: The project was approved by the local ethical committee in An- Najah National University.

References:

1. Jung D, Herrick R, Norman J, Turnlund K, Jan C, Feng K, et al. Impact of threading dislocation density on the lifetime of InAs quantum dot lasers on Si. Appl Phys Lett. 2018; 112(15): 153507
2. Klco N, Dumitrescu F, McCaskey A J, Morris T D, Pooser R C, Sanz M, et al. Quantum-classical computation of Schwinger model dynamics using quantum computers. Phys Rev A . 2018; 98(3): 032331.

3. van Veen J, Proutski A, Karzig T, Pikulin D I, Lutchyn R M, Nygård J, et al. Magnetic-field-dependent quasiparticle dynamics of nanowire single-Cooper-pair transistors. Phys Rev B. 2018; 98(17): 174502.
4. Kramer I J, Minor J C, Moreno Bautista G, Rollny L, Kanjanaboos P, Kopilovic D, et al. Efficient spray coated colloidal quantum dot solar cells. Adv Mater. 2005; 27(1):116-121.
5. Cross A W, Bishop L S, Sheldon S, Nation P D, Gambetta J M. Validating quantum computers using randomized model circuits. Phys Rev A. 2019; 100(3): 032328.
6. Vaseghi B, Rezaei G, Sajadi T. Optical properties of parabolic quantum dots with dressed impurity: combined effects of pressure, temperature and laser intensity. Physica B Condens Matter.2015 ; 456:171-175.
7. Bzour F, Shaer A, Elsaid M K. The effects of pressure and temperature on the exchange energy of a parabolic quantum dot under a magnetic field. J Taibah Univ Sci. 2017; 11(6): 1122-1134.
8. Ciftja O, Kumar A A. Ground state of two-dimensional quantum-dot helium in zero magnetic field: Perturbation, diagonalization, and variational theory. Phys Rev B. 2004; 70(20): 205326.
9. Ciftja O, Faruk M G. Two-dimensional quantum-dot helium in a magnetic field: Variational theory. Phys Rev B. 2005; 72(20): 205334.
10. Shaer A, Elsaid M K, Elhasan M. Variational calculations of the heat capacity of a semiconductor quantum dot in magnetic fields. Chin J Phys. 2016; 54(3): 391-397.
11. Kandemir B S. Variational study of two-electron quantum dots. Phys Rev B, 2005; 72(16): 165350.
12. Kandemir B S. Two interacting electrons in a uniform magnetic field and a parabolic potential: The general closed-form solution. J Math Phys. 2005; 46(3): 032110.
13. El-Said M. Spectroscopic structure of two interacting electrons in a quantum dot by the shifted 1/N expansion method. Phys Rev B. 2000; 61(19): 13026.
14. El-Said M. The energy level ordering in two-electron quantum dot spectra. Superlattice Microst. 1998; 23(6): 1237-1243.
15. Dybalski W, Hawrylak P. Two electrons in a strongly coupled double quantum dot: From an artificial helium atom to a hydrogen molecule. Phys Rev B. 2005; 72(20): 205432.
16. Khordad R, Tafaroji S, Katebi R, Ghanbari A. Optical and electronic properties of anisotropic parabolic quantum disks in the presence of tilted magnetic fields. Physica B Condens Matter. 2012 ; 407(3): 533-538.
17. Maksym P A, Chakraborty T. Quantum dots in a magnetic field: Role of electron-electron interactions. Phys. Rev. Lett. 1990; 65(1): 108.
18. Helle M, Harju A, Nieminen R M. Two-electron lateral quantum-dot molecules in a magnetic field. Phys Rev B. 2005; 72(20): 205329.
19. Phuc H V, Van Tung L. Linear and nonlinear phonon-assisted cyclotron resonances in parabolic quantum well under the applied electric field. Superlattice Microst. 2014; 71: 124-133.
20. Xin W, Zhao Y W. Effects of hydrogen-like impurity and electromagnetic field on quantum transition of an electron in a Gaussian potential with QD thickness. Superlattice Microst. 2018; 117: 220-227.
21. Semina M A, Golovatenko A A, Rodina A V. Ground state of the holes localized in II-VI quantum dots with Gaussian potential profiles. Phys Rev B. 2016; 93(4): 045409.
22. Boda A, Chatterjee A. Transition energies and magnetic properties of a neutral donor complex in a Gaussian GaAs quantum dot. Superlattice Microst. 2016; 97: 268-276.
23. Yuan J H, Chen N, Mo H, Zhang Y, Zhang Z H. The second harmonic generation in symmetrical and asymmetrical Gaussian potential quantum wells with applied electric field. Superlattices Microstruct. 2015; 88: 389-395.
24. Al-Hayek I, Sandouqa A S. Energy and binding energy of donor impurity in quantum dot with Gaussian confinement. Superlattice Microst. 2015; 85: 216-225.
25. Hong Z, Li-Xue Z, Xue W, Chun-Yuan Z, Jian-Jun L. Impurity-related electronic properties in quantum dots under electric and magnetic fields. Chin Phys B. 2011; 20(3): 037301.
26. Xie W. Optical properties of an off-center hydrogenic impurity in a spherical quantum dot with Gaussian potential. Superlattice Microst. 2010; 48(2): 239-247.
27. Elsaid M, Ali M, Shaer A. The magnetization and magnetic susceptibility of GaAs Gaussian quantum dot with donor impurity in a magnetic field. Mod Phys Lett B. 2019; 33(34): 1950422.
28. Ali M.The magnetization of single GaAs quantum dot with Gaussian confinement. Msc ,Thesis. Nablus: Najah National University; 2007,Available from: DSpace Repository.
29. Shaer A, ELSAID M, Elhasan M. The magnetic properties of a quantum dot in a magnetic field.Turk J Phy. 2016; 40(3): 209-218.
30. Nammas F S. Thermodynamic properties of two electrons quantum dot with harmonic interaction. Physica A. 2018; 508: 187-198.
31. Baghdasaryan D A, Hayrapetyan D B, Kazaryan E M, Sarkisyan H A. Thermal and magnetic properties of electron gas in toroidal quantum dot. Physica E Low Dimens Syst Nanostruct. 2018; 101: 1-4.
32. Hjaz E, Elsaid M K, Elhasan M. Magnetization of coupled double quantum dot in magnetic fields. J Comput Theor Nanos. 2017; 14(4): 1700-1705.
33. Elsaid M, Hjaz E, Shaer A. Energy states and exchange energy of coupled double quantum dot in a magnetic field. Int J Nano Dimens. 2017; 8(1): 1-8.
34. Elsaid M K, Hijaz E. Magnetic Susceptibility of Coupled Double GaAs Quantum Dot in Magnetic Fields. Acta Phys Pol A. 2017; 131(6).
35. Boyacioglu B, Chatterjee A. Magnetic properties of semiconductor quantum dots with gaussian confinement. Int J Mod Phys B. 2012; 26(4): 1250018.

36. Nguyen N T, Sarma S D. Impurity effects on semiconductor quantum bits in coupled quantum dots. Phys Rev B. 2011; 83(23): 235322.
37. Boyacioglu B, Chatterjee A. Heat capacity and entropy of a GaAs quantum dot with Gaussian confinement. J appl. Phys. 2012; 112(8): 083514.

أطياف الطاقة و السعة الحرارية لنقطة كمية من زرنخيد الجاليوم موضوعة في مجال مغناطيسي خارجي

محمود علي محمد السعيد أيهم شاعر

قسم الفيزياء، كلية العلوم، جامعة النجاح الوطنية، نابلس، الضفة الغربية، فلسطين.

الخلاصة:

تم دراسة أطياف الطاقة والسعة الحرارية لإلكترون مفرد محصور في نقطة كمية وموضوع في مجال مغناطيسي خارجي منتظم باستخدام نموذج جاوس كجهد حصر. تم استخدام طريقة المحاور الدقيقة لحل دالة هاميلتون لنقطة الكم الكاوسية مع الأخذ بعين الاعتبار الحركة المغزلية للإلكترون. جميع عناصر مصفوفة الطاقة تم حسابها بصورة مجموع منتهي. تم عرض اعتماد أطياف الطاقة للإلكترون كدالة للمجال المغناطيسي ، وشدة جهد الحصر الكاوسي وحجم النقطة الكمية. بالإضافة إلى ذلك، تم دراسة سلوك السعة الحرارية للنقطة الكمية كدالة لدرجة الحرارة و المجال المغناطيسي الخارجي المؤثر عليها.

الكلمات المفتاحية : نقطة كمية كاوسية ، أطياف الطاقة ، طريقة الأقطار الدقيقة ، السعة الحرارية